The PACE-MAPP Polarized Ocean Bio-optical Model

James Allen, Snorre Stamnes, Eduard Chemyakin, Grant Sims, Michael Jones, Adam Bell, Jacek Chowdhary, Brian Cairns

1. Abstract

The MAPP polarimeter retrieval algorithm, originally developed for the airborne NASA GISS Research Scanning Polarimeter, is being adapted to the PACE observing system to allow for a simultaneous retrieval of **aerosol**, **thin cirrus**, and **ocean products** using both PACE polarimeters and the OCI shortwave infrared channels. Here, we describe the **polarized ocean bio-optical model** we have developed for PACE-MAPP, which is designed to use a combination of **homogenous** and **coated spheres** to more accurately model the absorption and backscattering properties of algal and non-algal particles, and which also includes absorption by colored dissolved organic matter.

We first use Lorenz-Mie computations to create lookup tables to accurately and efficiently characterize the optical properties of homogeneous and coated spheres embedded in water for PACE. We then use these lookup tables to develop a bio-optical model that consists of an external mixture of **homogeneous (non-algal)** and **coated (algal) spheres**. Lastly, we use the bio-optical model in forward radiative transfer computations to perform inversions of MODIS remote sensing reflectance for a variety of ocean regions. We explore the sensitivity of these inversions to ocean constituent inherent optical properties.

2. Power-Law Size Distribution Properties

- Power-Law Range: 2.5 – 6

Non-algal Particles

- Homogenous Spheres
- Minimum Radius: 0.01 um
- Maximum Radius: 100 um

Algal Particles

- Coated Spheres
- Minimum Radius: 0.15 um
- Maximum Radius: 30 um
- Core to Shell Diameter Ratio: 85%

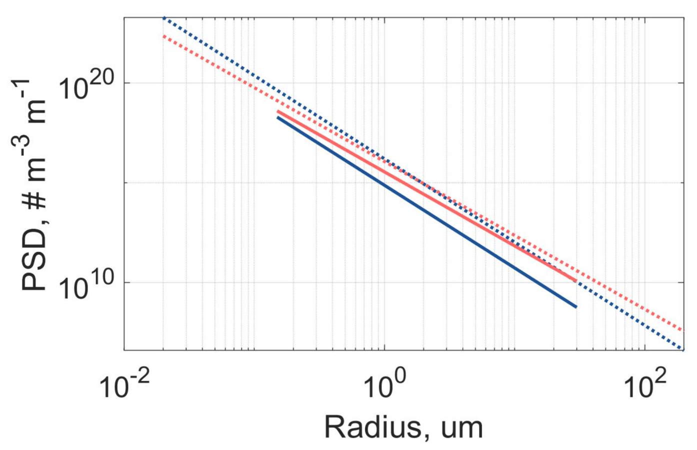

Figure 1. Particle size distributions of algal (solid lines) and non-algal (dotted lines) for retrievals from Station ALOHA (blue) and the North Atlantic Bloom Experiment (red) station locations for April 2006.

3. Optical Properties

Non-algal Particles

Whole-Particle Refractive Index		
Real Part	n	[1.05 – 1.2]
Imaginary Part	n'	$0.010658\ e^{-0.007186\,\lambda}$

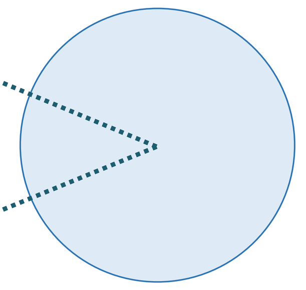

- Constant real refractive index
- Imaginary component varies with wavelength as exponential decay function (Stramski et al., 2004)

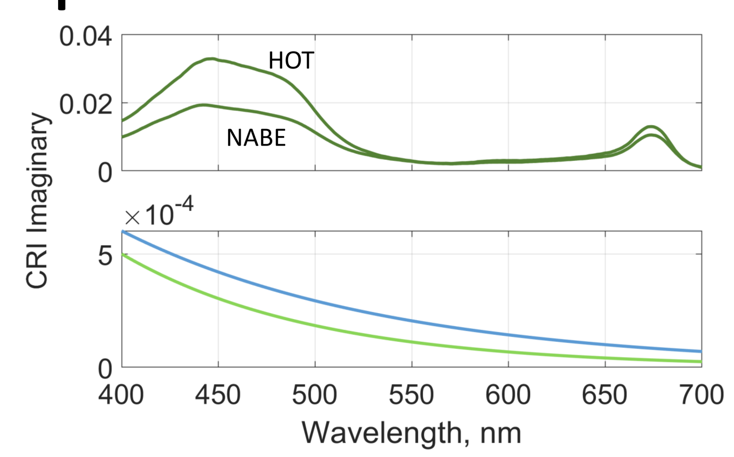

Figure 2. Retrievals of the Imaginary part of the complex refractive index as a function of wavelength for non-algal particles (blue), algal cores (light green), and algal shells for 1um-radius algal particles (dark green).

Algal Particles

Cytoplasm Core		
Relative Volume	V	61%
Real Part	n	1.02
Imaginary Part	n'	$0.0005\ e^{-0.01\,(\lambda - 400)}$

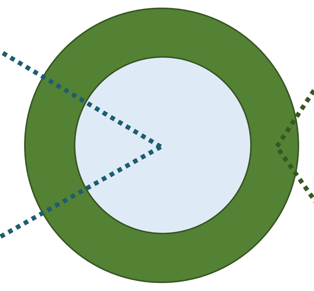

Pigment Shell		
Relative Volume	V	39%
Real Part	n	1.05 – 1.2
Imaginary Part	n'	f([chl], r, chlDens)

- Constant real refractive index for cytoplasm core
- Core imaginary component varies with wavelength as exponential decay function (Bernard et al., 2009)
- Constant retrieved shell real refractive index
- Imaginary component is a function of an input chlorophyll concentration, particle radius, and the interstitial chlorophyll concentration (Morel and Bricaud, 1986)
  - Phytoplankton specific absorption as f([chl]) (Bricaud et al., 1998)
  - Package effect parameterization from size and interstitial chl (Finkel et al., 2004; Morel and Bricaud, 1981)

4. Station Retrievals

BOM Inputs	Station ALOHA: Chl = 0.068	North Atlantic Bloom Experiment: Chl = 0.261
Non-algal Particles		
PSD slope	4.17	3.7
Relative Volume, percent	71	30
Real CRI	1.12	1.1
Algal Particles		
PSD Slope	4.14	3.71
Relative Volume, percent	29	70
Interstitial Chl, kg m^{-1}, (1 um)	3.01	3.16
Shell Real CRI	1.11	1.11
CDOM absorption at 443nm	0.0055	0.0261

Table of bio-optical model inputs, to be used with constants from Sections 2 and 3.

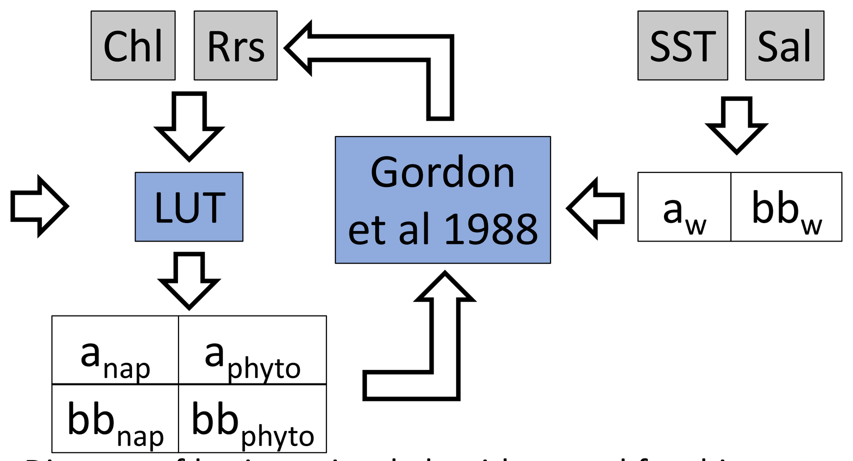

Diagram of basic retrieval algorithm used for this poster. Chlorophyll was used with the bio-optical model inputs and the Lorenz-Mie Lookup Table to derive optical parameters, which were used with water optical parameters derived from sea surface temperature and salinity to minimize the difference in calculated remote sensing reflectance and the satellite input.

5. Inherent Optical Properties Results

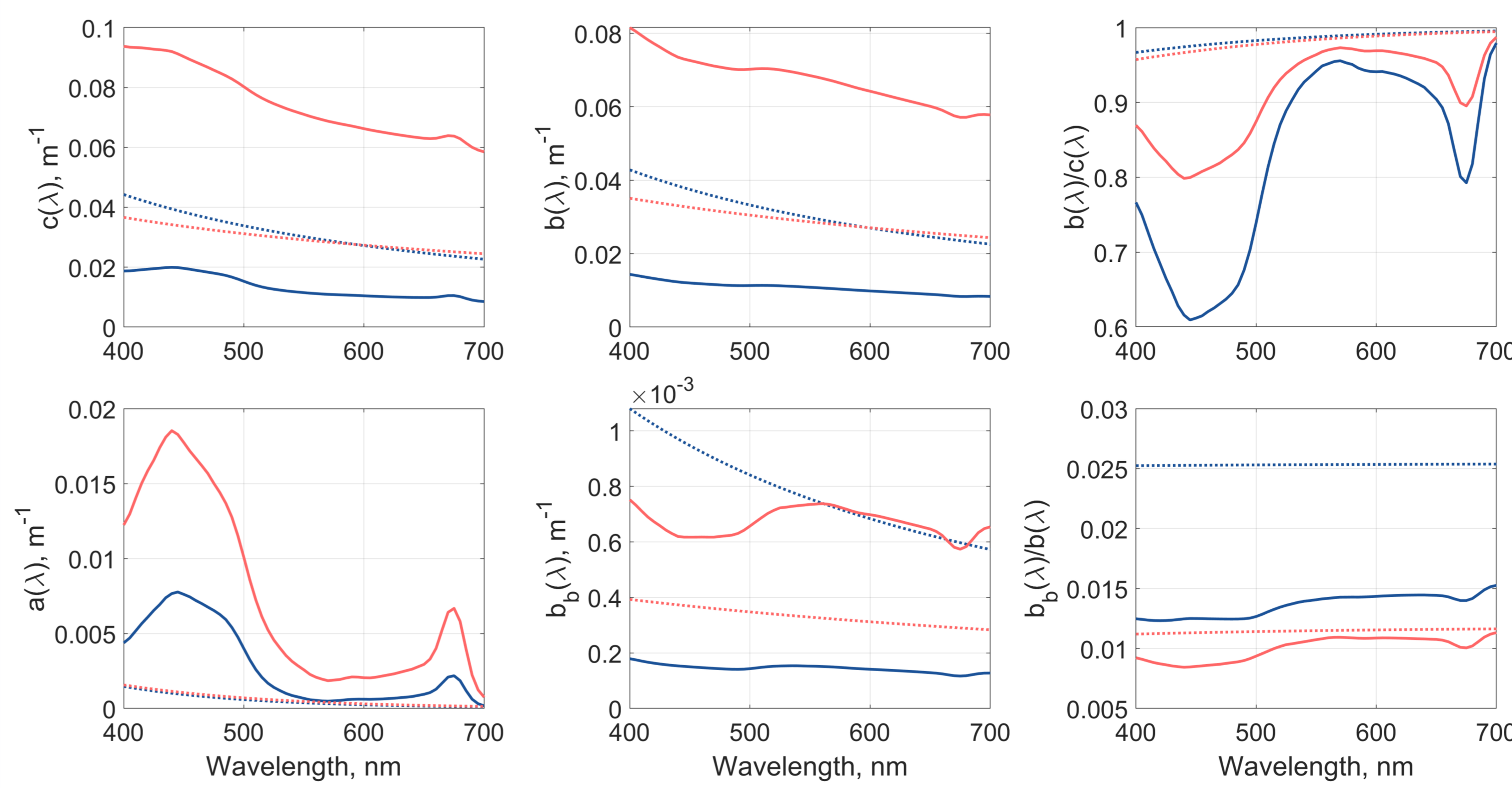

Figure 3. Retrievals of the particulate beam attenuation c(λ), total scattering (b(λ)), single scattering albedo b(λ)/c(λ), absorption a(λ), backscattering $b_b(\lambda)$, and the backscattering ratio $b_b(\lambda)/b(\lambda)$ for the algal (solid line) and non-algal (dotted line) particle population at the Station ALOHA (blue) and the North Atlantic Bloom Experiment (red) stations for April 2006.

6. Polarization Properties Results

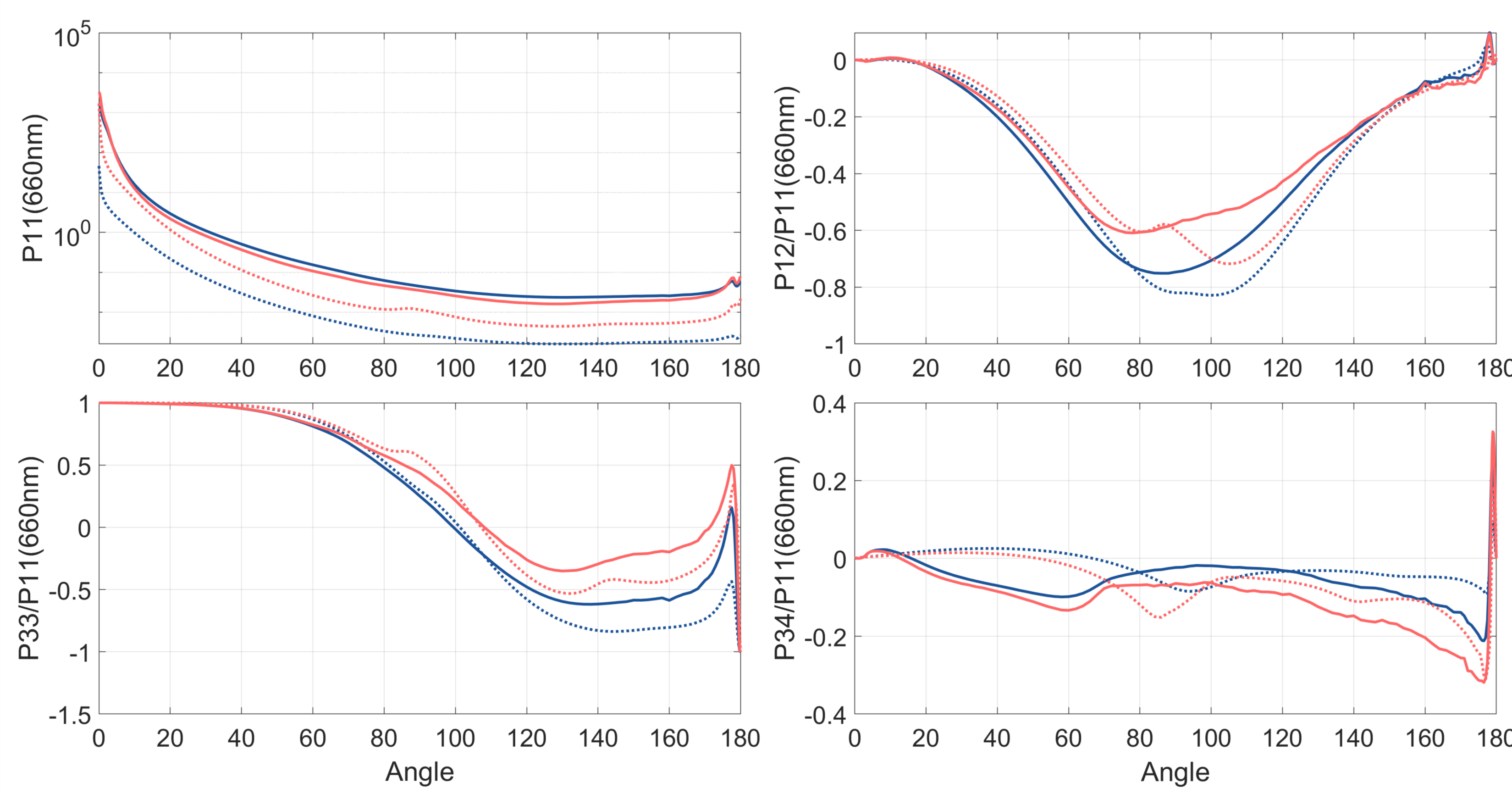

Figure 4. Derivations of the volume scattering function normalized by total scattering (P11), and each of the scattering phase matrix components normalized by P11 for Station ALOHA (blue) and the North Atlantic Bloom Experiment (red) stations for April 2006.

7. Neural Network Speed Boost

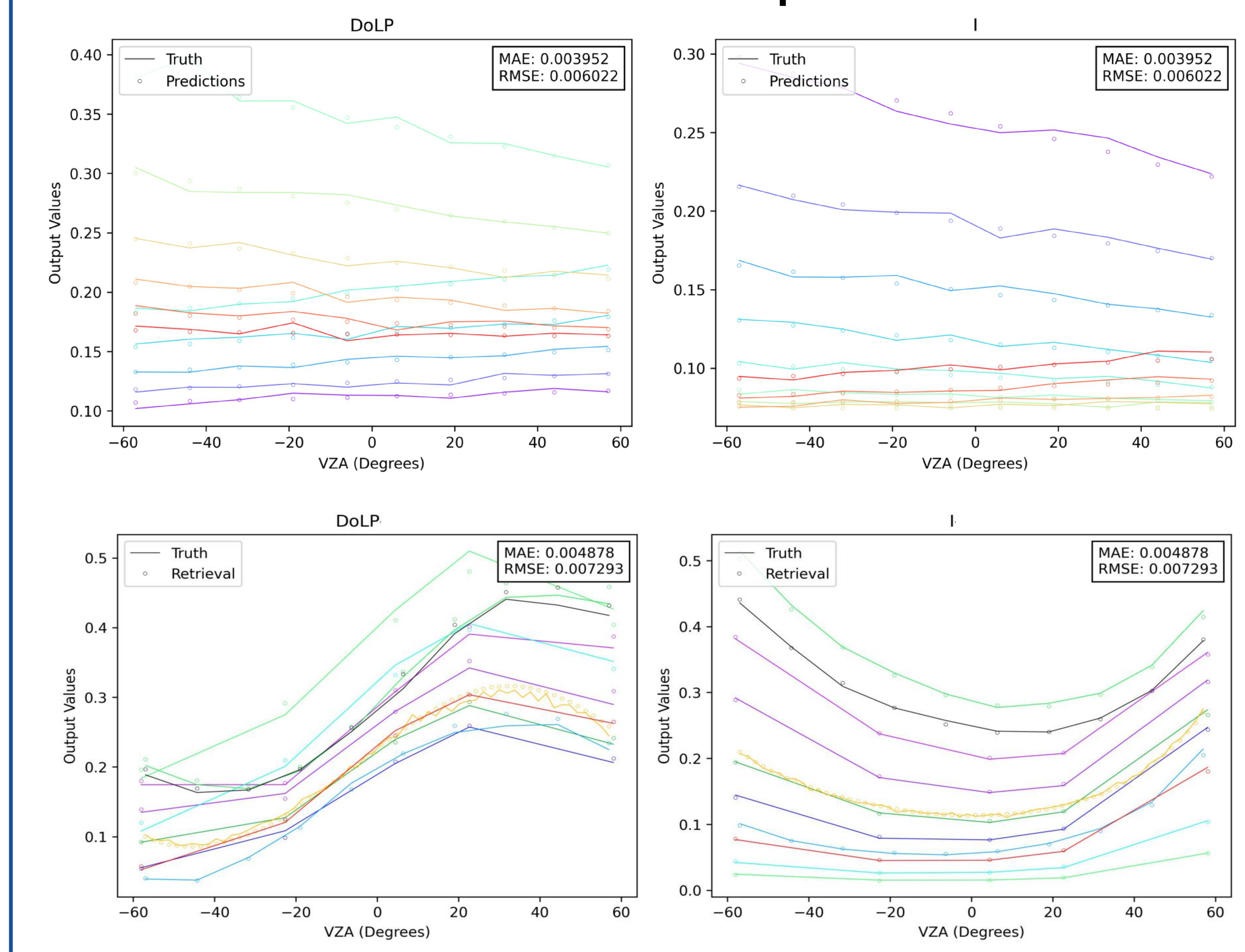

Neural network for each of three particle populations:

- Homogeneous non-algal particles
- Coated algal particles with single complex refractive index
- Coated algal particles with size-dependent complex refractive index

Neural network version of the bio-optical model is 1000x faster

8. Takeaways

- Our new bio-optical model retrieves the spectral optical properties and scattering phase matrix of algal and non-algal particles
- Algal particles are modeled as coated spheres with a cytoplasm core and a pigment shell; non-algal particles are modeled as homogeneous spheres
- Our bio-optical model allows for wavelength- and size-dependent complex refractive indices for a more mechanistic retrieval of ocean constituents
- Our bio-optical model can improve satellite remote sensing and in-situ retrievals of ocean properties with minimal computational effort

9. References

Bernard, S., T. A. Probyn, and A. Quirantes. 2009. Simulating the optical properties of phytoplankton cells using a two-layered spherical geometry. Biogeosciences Discuss. **6**: 1497–1563. doi:10.5194/bgd-6-1497-2009

Bricaud, A., A. Morel, M. Babin, K. Allali, and H. Claustre. 1998. Variations of light absorption by suspended particles with chlorophyll *a* concentration in oceanic (case 1) waters: Analysis and implications for bio-optical models. J. Geophys. Res. **103**: 31033–31044. doi:10.1029/98JC02712

Finkel, Z., A. Irwin, and O. Schofield. 2004. Resource limitation alters the 3/4 size scaling of metabolic rates in phytoplankton. Mar. Ecol. Prog. Ser. **273**: 269–279. doi:10.3354/meps273269

Gordon, H. R., O. B. Brown, R. H. Evans, J. W. Brown, R. C. Smith, K. S. Baker, and D. K. Clark. 1988. A semianalytic radiance model of ocean color. J. Geophys. Res. **93**: 10909. doi:10.1029/JD093iD09p10909

Morel, A., and A. Bricaud. 1981. Theoretical results concerning light absorption in a discrete medium, and application to specific absorption of phytoplankton. Deep Sea Research Part A. Oceanographic Research Papers **28**: 1375–1393. doi:10.1016/0198-0149(81)90039-X

Morel, A., and A. Bricaud. 1986. Inherent properties of algal cells including picoplankton: Theoretical and experimental results. Canadian Bulletin of Fisheries and Aquatic Sciences **214**: 521–559.

Stamnes, S., C. Hostetler, R. Ferrare, et al. 2018. Simultaneous polarimeter retrievals of microphysical aerosol and ocean color parameters from the "MAPP" algorithm with comparison to high-spectral-resolution lidar aerosol and ocean products. Appl. Opt., AO **57**: 2394–2413. doi:10.1364/AO.57.002394

Stramski, D., E. Boss, D. Bogucki, and K. J. Voss. 2004. The role of seawater constituents in light backscattering in the ocean. Progress in Oceanography **61**: 27–56. doi:10.1016/j.pocean.2004.07.001